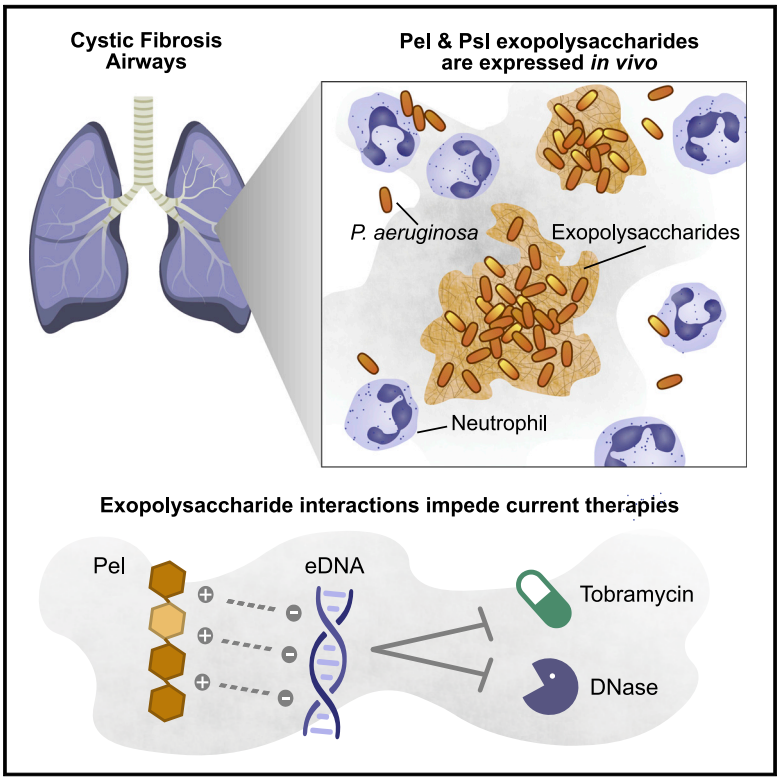
Cell Reports

Pseudomonas aeruginosa aggregates in cystic fibrosis sputum produce exopolysaccharides that likely impede current therapies

Graphical Abstract



Highlights

- Pel and Psl are produced by *P. aeruginosa* aggregates in cystic fibrosis sputum
- Attributes of *in vitro* biofilms are seen in clinical aggregates
- Aggregate morphology is consistent with polysaccharide-dependent aggregation
- Pel-DNA interactions reduce susceptibility to antibiotic and mucolytic treatments

Authors

Laura K. Jennings, Julia E. Dreifus, Courtney Reichhardt, ..., Daniel J. Wozniak, Katherine B. Hisert, Matthew R. Parsek

Correspondence

parsem@u.washington.edu

In brief

Pseudomonas aeruginosa forms biofilm aggregates in cystic fibrosis airways. Jennings et al. demonstrate that Pel and Psl exopolysaccharides are produced by *P. aeruginosa* in cystic fibrosis sputum and that aggregates are consistent with a polysaccharide-dependent aggregation mechanism. Exopolysaccharide interactions with extracellular DNA increase antimicrobial tolerance and protect DNA from digestion.

Jennings et al., 2021, Cell Reports *34*, 108782
February 23, 2021 © 2021 The Authors.
https://doi.org/10.1016/j.celrep.2021.108782

CellPress

Cell Reports

CellPress
OPEN ACCESS

Report

Pseudomonas aeruginosa aggregates in cystic fibrosis sputum produce exopolysaccharides that likely impede current therapies

Laura K. Jennings,[1,6] Julia E. Dreifus,[1] Courtney Reichhardt,[1] Kelly M. Storek,[1,7] Patrick R. Secor,[1,6] Daniel J. Wozniak,[2,3,4] Katherine B. Hisert,[5,8] and Matthew R. Parsek[1,9,*]

[1]Department of Microbiology, University of Washington, Seattle, WA 98195, USA
[2]Department of Microbial Infection and Immunity, The Ohio State University, Columbus, OH 43210, USA
[3]Department of Microbiology, The Ohio State University, Columbus, OH 43210, USA
[4]Infectious Disease Institute, The Ohio State University, Columbus, OH 43210, USA
[5]Department of Medicine, University of Washington, Seattle, WA 98195, USA
[6]Present address: Division of Biological Sciences, University of Montana, Missoula, MT 59812, USA
[7]Present address: Department of Infectious Diseases, Genentech Inc., South San Francisco, CA 94080, USA
[8]Present address: Department of Medicine, National Jewish Health, Denver, CO 80206, USA
[9]Lead contact
*Correspondence: parsem@u.washington.edu
https://doi.org/10.1016/j.celrep.2021.108782

SUMMARY

In cystic fibrosis (CF) airways, *Pseudomonas aeruginosa* forms cellular aggregates called biofilms that are thought to contribute to chronic infection. To form aggregates, *P. aeruginosa* can use different mechanisms, each with its own pathogenic implications. However, how they form *in vivo* is controversial and unclear. One mechanism involves a bacterially produced extracellular matrix that holds the aggregates together. Pel and Psl exopolysaccharides are structural and protective components of this matrix. We develop an immunohistochemical method to visualize Pel and Psl in CF sputum. We demonstrate that both exopolysaccharides are expressed in the CF airways and that the morphology of aggregates is consistent with an exopolysaccharide-dependent aggregation mechanism. We reason that the cationic exopolysaccharide Pel may interact with some of the abundant anionic host polymers in sputum. We show that Pel binds extracellular DNA (eDNA) and that this interaction likely impacts current therapies by increasing antimicrobial tolerance and protecting eDNA from digestion.

INTRODUCTION

Cystic fibrosis (CF) is caused by mutations in the gene encoding the CF transmembrane conductance regulator (CFTR), a membrane anion channel (Stoltz et al., 2015). The vast majority of individuals with CF will eventually become chronically infected with the Gram-negative pathogen *Pseudomonas aeruginosa* (Lyczak et al., 2002; Moreau-Marquis et al., 2008). Persistence of CF airway infections is associated with non-resolving inflammation, accelerated lung disease, and earlier mortality (Gibson et al., 2003; Lyczak et al., 2002). *In vitro* antibiotic susceptibility of *P. aeruginosa* clinical isolates by itself does not predict treatment outcomes (Somayaji et al., 2019). Thus, it is not clear which host and microbiological factors influence antibiotic efficacy.

In the CF airways, *P. aeruginosa* is thought to reside as a biofilm or aggregate of cells embedded in a polymer-rich matrix (Bjarnsholt et al., 2009; Costerton et al., 1995; Singh et al., 2000). Exopolysaccharides (EPSs) are key components of this matrix (Flemming and Wingender, 2010; Pamp et al., 2007; Sutherland, 2001). *P. aeruginosa* is capable of producing at least three distinct matrix EPSs: alginate, Psl, and Pel (Franklin et al., 2011). Alginate is the primary EPS used by mucoid strains. Nonmucoid clinical and environmental isolates vary the amount and type of EPSs that they produce (Colvin et al., 2012; Ma et al., 2006). Psl is a neutral polymer containing mannose, glucose, and rhamnose in a repeating pentameric unit (Byrd et al., 2009). *In vitro*, Psl facilitates surface adherence and proinflammatory signaling in lung epithelial cells (Byrd et al., 2010) and inhibits opsonization and bacterial killing by phagocytes (Mishra et al., 2012). Pel, a polycationic polymer composed of partially acetylated glucosamine and galactosamine (Jennings et al., 2015), can bind extracellular DNA (eDNA) via an ionic binding mechanism (Jennings et al., 2015) and play an additional protective role by enhancing resistance to aminoglycoside antibiotics (Colvin et al., 2011). Whether *in vivo P. aeruginosa* aggregates produce Pel and Psl, or any other features of the matrix described *in vitro*, remains unknown.

However, recent reports suggest that *in vitro* findings regarding *P. aeruginosa* aggregate formation may not apply to aggregates produced during chronic infection (Bjarnsholt et al., 2013). For example, some studies found that functions that contribute to aggregate formation *in vitro* are not required

This is an open access article under the CC BY-NC-ND license (http://creativecommons.org/licenses/by-nc-nd/4.0/).

to produce aggregates under conditions that mimic the CF environment. Staudinger et al. (2014) showed that *P. aeruginosa* growing in a viscous medium *in vitro* could produce aggregates independent of EPS production. These aggregates exhibited many of the phenotypic attributes associated with matrix-mediated aggregation. Subsequently, Secor et al. (2018) demonstrated that a polymer-rich environment (like that found in the CF airways) could drive bacterial aggregation through a passive mechanism termed depletion aggregation. Depletion aggregation occurs in environments where bacterial aggregation reduces the entropy of the system by providing more space for the polymers. Collectively, these data call into question the relevance of some *in vitro* biofilm findings to chronic CF airway infections and highlight the importance of studying aggregates generated in the human disease environment.

In this study, we apply immunohistochemistry (IHC) using antibodies specific to Pel and Psl EPSs to directly visualize the *P. aeruginosa* biofilm matrix in CF sputum. We provide evidence that Pel and Psl are produced in the CF airways. We demonstrate that Pel is partially acetylated and has a positive charge at CF-relevant airway pH. This charge allows Pel to bind an abundant host component of the airways, eDNA. The presence of Pel-bound eDNA increased tolerance to aminoglycoside antibiotics. Moreover, the ability of Pel to bind eDNA protects the polymer from DNase digestion. Collectively, our data indicate that, in CF, a subpopulation of *P. aeruginosa* produces aggregates expressing Pel and/or Psl EPSs. This finding is significant. It shows that aggregate growth *in vivo* is consistent with the biofilm mode of growth as defined by *in vitro* laboratory research. Our work also suggests that Pel produced by aggregates likely diminishes the efficacy of the most commonly used current CF therapeutics: inhaled tobramycin and DNase. Thus, patient-to-patient differences in EPS production by bacterial aggregates could help explain the heterogeneous responses to these therapies in the clinic.

RESULTS

CF isolates of *P. aeruginosa* have the genetic capacity for Pel and Psl production

Sputum samples were collected with consent from eight CF patients at the University of Washington (UW) Adult CF Clinic. Five sputum samples (hereafter indicated as P1–P5) were identified to contain *P. aeruginosa* using culture-based techniques. Three control sputum samples (C1–C3) did not contain detectable levels of *P. aeruginosa*. Clinical descriptions of patient samples are listed in Table S1.

We verified the presence or absence of *P. aeruginosa* in sputum samples using endpoint PCR with *P. aeruginosa*-specific primers. We probed sputum samples for the presence of genomic DNA harboring *pel* or *psl* genes (Figure S1). We found that all sputum samples that contained *P. aeruginosa* also tested positive for *pel* genes and that *psl* genes were detected in four of five samples, suggesting that the genetic capability of sputum pathogens to produce these EPSs varies between patients. As expected, *pel* and *psl* genes were not detected in the control samples.

Pel and Psl are associated with *P. aeruginosa* aggregates in CF sputum

We next sought to determine whether EPSs were being produced in sputum samples. Toward this end, we used IHC with antibodies directed specifically to the Pel and Psl EPSs. These antibodies were validated and optimized by spiking EPS-producing cells into sputum samples lacking *P. aeruginosa* (Figures S2A and S2B). We then applied our IHC assay to sputum samples obtained from people with CF that we had documented to contain *P. aeruginosa* (Figure 1). All samples contained abundant neutrophils in which the multi-lobed nuclei stained dark blue due to the hematoxylin counterstain, which is consistent with an intense inflammatory response in the CF airways that fails to clear the infection (Cantin et al., 2015). Visualization of *P. aeruginosa* in these samples showed abundant single cells and small aggregates as well as a few larger aggregates. Pel, Psl, or both were associated with *P. aeruginosa* clusters and detected in all of the clinical specimens containing *P. aeruginosa* (see *P. aeruginosa* aggregates in sputum indicate heterogeneity in aggregate size and matrix composition). Dual staining of Pel and *P. aeruginosa* illustrated some aggregates in which the matrix extends beyond cell clusters, similar to *in vitro* biofilms (Figure 1A). In many cases, some of the larger aggregates appeared to consist of several smaller clusters separated by matrix material (Figure 1B, second panel from left).

P. aeruginosa aggregates in sputum indicate heterogeneity in aggregate size and matrix composition

Abundant single cells and small aggregates, as well as a few larger aggregates, were visible (Figure 1C). Cluster size analysis of *P. aeruginosa* aggregates was conducted on five sputum samples and compared with biofilm aggregates of clinical and environmental isolates of *P. aeruginosa* (PAO1, PA14, MSH3, and 19660) cultivated *in vitro* under continuous flow as described by Colvin et al. (2012). Overall, *in vivo* aggregates in sputum are smaller than aggregates commonly observed in *in vitro* studies (Figure 1D). The upper limit of sputum aggregates was ~300 μm (compared with 150 μm for flow cells), with the most abundant number of aggregates in the smallest size range (<20 μm). By contrast, flow cell aggregates were more uniform in size.

Analysis of IHC images by visual inspection showed the presence or absence of Pel and Psl in sputum samples (Figures 2A and 2B). Pel was detected in all five *P. aeruginosa*-positive sputum samples tested (P1–P5). Psl was detected in three of five *P. aeruginosa*-positive sputum samples (P1, P3, and P5). Pel and Psl were not detected in controls without *P. aeruginosa* (C1–C3). Detection of Pel and Psl in sputum by IHC was consistent with PCR results. Gram-positive cocci, which were presumably *Staphylococcus*, did not stain with *P. aeruginosa*, Pel, or Psl antibodies (Figure S2C). In addition to detecting Pel and Psl by visual inspection, we sought to objectively quantify the antibody signal using VisioPharm image analysis software. A global quantification of antibody signal across the entire slide could be used to determine the presence/absence of the target antigen for controls (Figure S2B) and most sputum samples (Figure 2C). Quantification with VisioPharm has its limitations. The main limitation is that it is challenging to detect polysaccharides in samples with only a few

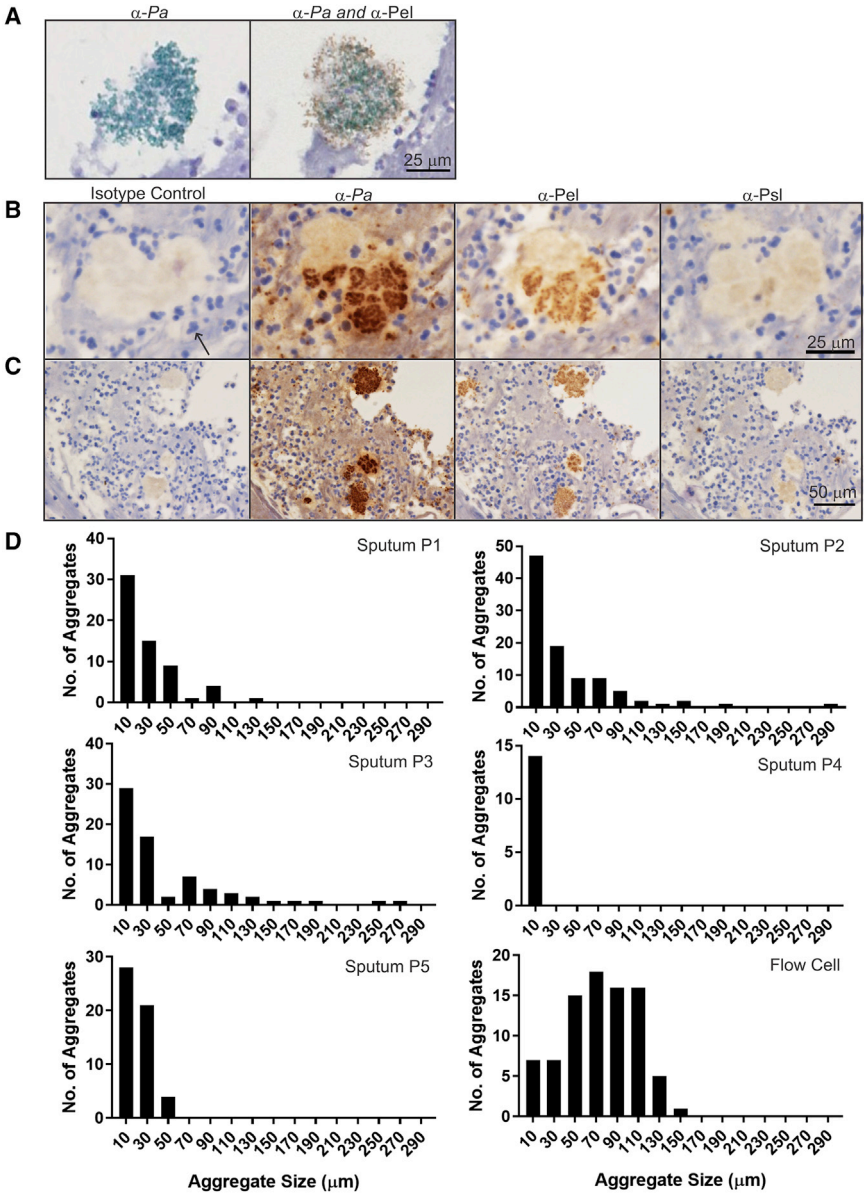


Figure 1. Characteristics and observations of the *in vivo* biofilm matrix

(A) Dual IHC staining of a sputum aggregate showing Pel (brown) and *P. aeruginosa* (green).

(B and C) Representative IHC images of Pel, Psl, and *P. aeruginosa* (*Pa*) antibodies (brown) applied to sequential slices of *Pa*-positive sputum. Hematoxylin counterstain is blue. A neutrophil is highlighted (arrow).

(B) Images showing larger *Pa* cell cluster that appears to consist of several smaller clusters.

(C) Images showing heterogeneity in *Pa* cell cluster size.

(D) Size distribution of Pa aggregates in sputum samples (P1–P5) and *in vitro* flow-cell biofilms from reference Colvin et al. (2012).

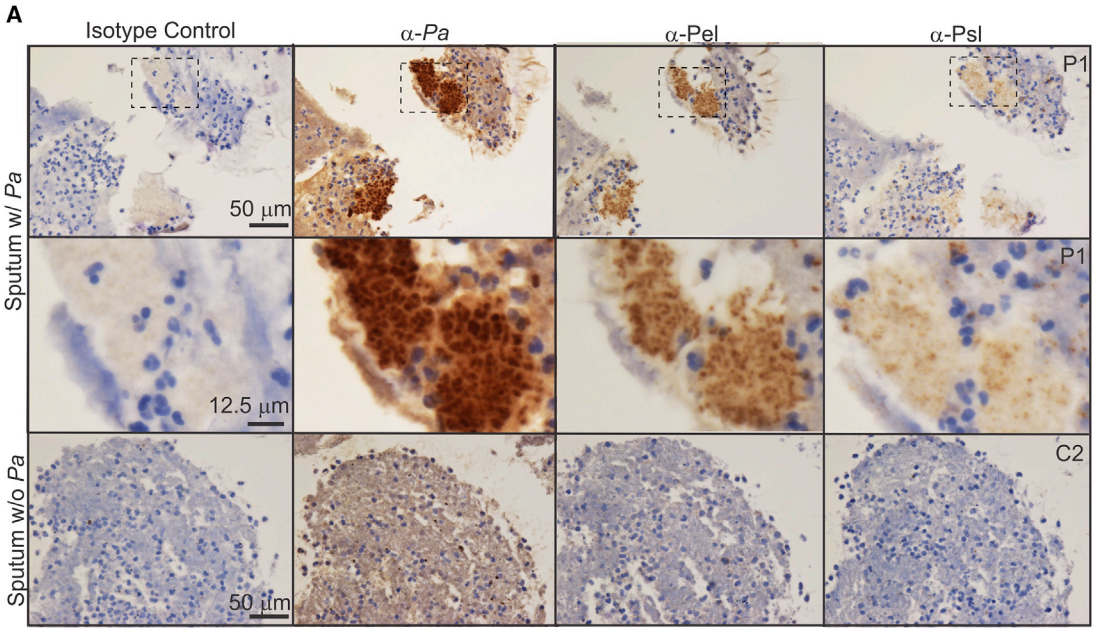
aggregates staining. For these reasons, the global quantification method likely results in an underestimation of EPS detection. Within sputum samples, most *P. aeruginosa* aggregates stained positive for Pel, Psl, or both (Figure 2D). In the samples that we tested, Pel staining is more prevalent than Psl staining. Overall, our analysis indicates all sputum samples contained at least one EPS and that the expression of Pel and Psl can vary between patients.

Cellular orientation within clusters suggests aggregation occurs by an EPS-mediated polymer-bridging mechanism

Bacterial aggregation can occur by different mechanisms: restricted motility (Staudinger et al., 2014), depletion aggregation (Dorken et al., 2012; Schwarz-Linek et al., 2010; Secor et al., 2018), and polymer bridging (Strand et al., 2003). The morphology of aggregates in the sputum samples can be used to distinguish between different mechanisms of aggregation (Secor et al., 2018). Non-motile cells produce aggregates that are densely packed and uniformly distributed throughout the aggregate, compared with polymer bridging in which aggregates have a higher cell density in the center with fewer cells toward the edges (Staudinger et al., 2014). In depletion aggregation, rod-shaped bacteria laterally align to minimize aggregate surface area (Figure 2E, bottom left) (Secor et al., 2018), compared with the less ordered orientation of cells aggregated by polymer bridging (Figure 2E, bottom right). IHC reveals that *P. aeruginosa* cells in sputum are not laterally aligned and that the cell density is greater toward the center of most clusters (Figure 2E, top). The cellular packing and orientation of *P. aeruginosa* within aggregates in sputum are consistent with a polymer-bridging mechanism.

Pel is highly deacetylated and aggregates CF-relevant polymers and sputum in a pH-dependent manner *in vitro*

The evidence that Pel and Psl are produced by *P. aeruginosa* in the CF airways raises the possibility that these EPSs might mediate functionally important interactions with host-derived airway components. Of particular interest is Pel, which is polycationic and could potentially contribute to interactions in airways that are rich in host-derived anionic constituents. Our previous work showed that Pel was enriched in 1,4-glycosidic linkages of *N*-acetylgalactosamine (GalNAc) and *N*-acetylglucosamine (GlcNAc) sugars (Jennings et al., 2015). Deacetylation of Pel



B

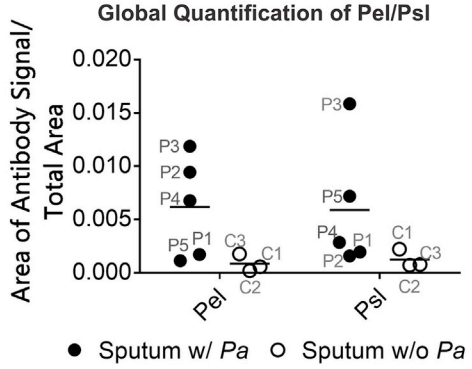
Qualitative Detection of Pel/Psl by Visual Inspection

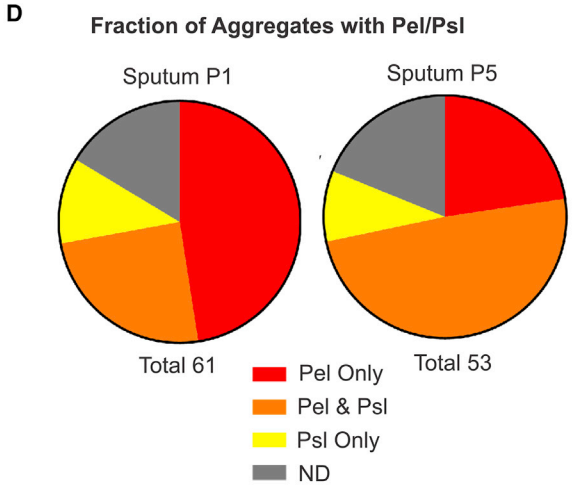
Pa-Positive Sputum

ID	Pel	Psl
P1	+	+
P2	+	-
P3	+	+
P4	+	-
P5	+	+

Pa-Negative Sputum

ID	Pel	Psl
C1	-	-
C2	-	-
C3	-	-





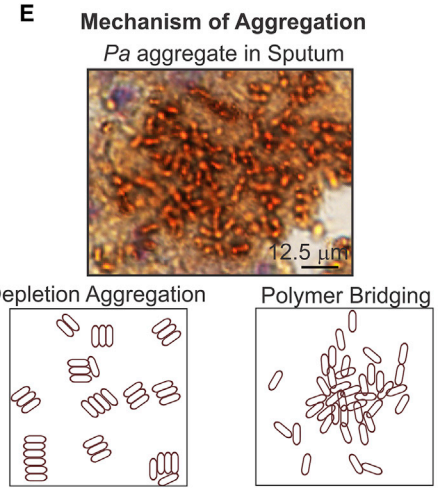


Figure 2. IHC indicates presence and localization of Pel and Psl in CF sputum

(A) Representative IHC images of Pel, Psl, and Pa antibodies (brown) applied to sequential slices of sputum with *Pa* (P1) and sputum without *Pa* (C2).
(B) Qualitative detection of Pel or Psl in sputum by visual inspection. +, detected; –, not detected.
(C) Global quantification of the area of antibody signal/total area of sample for sputum samples.
(D) Fraction of aggregates within a sputum sample with Pel or Psl. ND, aggregate not detected; Total, number of aggregates.
(E) Representative image showing morphology of *Pa* aggregates in sputum is consistent with a polymer-bridging mechanism.

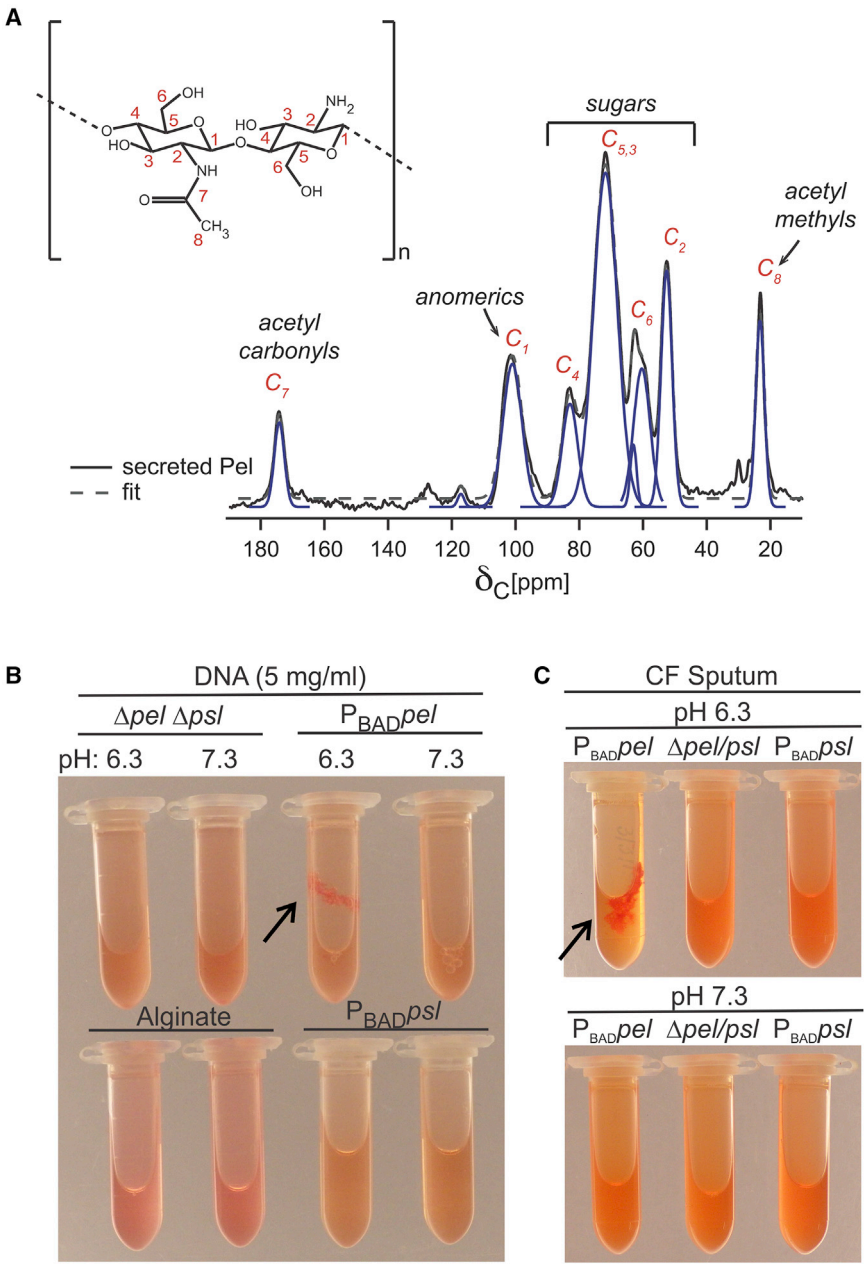


Figure 3. Pel is highly deacetylated and aggregates CF-relevant polymers in a pH-dependent manner

(A) NMR structural analysis of Pel is consistent with a 50% acetylated polymer of GlcNAc and GalNAc. The ^{13}C-CPMAS spectrum of Pel was acquired and compared with poly-β-1,4-GlcNAc (inset). Biological replicate spectra shown in Figure S3C.

(B) Pel, but not Psl or alginate, binds eDNA. Supernatant from P_{BAD}*pel* culture combined with salmon sperm DNA forms a large aggregate (arrow) at pH 6.3, where Pel is positively charged. Aggregation did not occur for supernatant from P_{BAD}*psl* or alginate solution or no polysaccharide control (Δ*pel* Δ*psl*).

(C) Pel aggregates CF sputum at pH 6.3 (arrow).

(B and C) Representative images shown for clarity. Triplicate biological replicates behaved similarly.

sugars by the enzyme PelA results in its overall positive charge (Colvin et al., 2013).

Previous attempts to apply solution NMR to Pel were hindered by the polymer's limited solubility. To assess the degree of deacetylation, we applied solid-state NMR to Pel from a Pel-overproducing strain (PAO1 Δ*wspF* Δ*psl* P_{BAD}*pel*), herein designated as P_{BAD}*pel* (Jennings et al., 2015). The ^{13}C cross-polarization magic-angle spinning (^{13}C-CPMAS) NMR spectrum of Pel was acquired (Figures 3A and S3C) and contained peaks consistent with GlcNAc/GalNAc (Vårum et al., 1991). To determine the extent of Pel deacetylation, the CP contact time was arrayed, which permitted quantitative peak integration (Figures S3A and S3B). This experiment determined that there is ~0.5 acetyl group per sugar. The extent of deacetylation of Pel is greater than that observed for poly-*N*-acetylglucosamine (PNAG) produced by *Staphylococcus* spp. (10%–20% deacetylated) (Little et al., 2014).

Based on the high degree of deacetylation determined from NMR, we reasoned that Pel would bind anionic polymers in the CF airways (Fischer and Widdicombe, 2006). The pH of the CF airways is mildly acidic (pH 6.0) (Coakley et al., 2003) and would impart a positive charge on Pel, facilitating the formation of ionic interactions. In addition, we had evidence that Pel can bind to both DNA and mucin, which are some of the most abundant anionic polymers in CF sputum (Button et al., 2012; Mrsny et al., 1996; Shak et al., 1990). To follow up on these observations, we wanted to verify that it was Pel that bound eDNA and not any other exopolymers that *P. aeruginosa* produces. Therefore, we analyzed the ability of the additional *P. aeruginosa* EPS Psl and alginate to interact with eDNA. As previously reported, pH-dependent aggregation (due to binding) was observed when positively charged Pel was mixed with salmon sperm DNA (Figure 3B). No aggregation was observed with alginate, Psl, or a polysaccharide-free control (Δ*pel* Δ*psl*) at either pH tested. Pel and Psl immunoblots suggest Pel and Psl supernatants had similar amounts of polysaccharide (Figure S3D). Next, we sought to determine whether Pel could directly aggregate macromolecules present in sputum recovered from a person with CF. We found that Pel aggregated sputum in a pH-dependent manner, while no aggregation was observed for Psl or a polysaccharide-free control (Δ*pel* Δ*psl*) (Figure 3C).

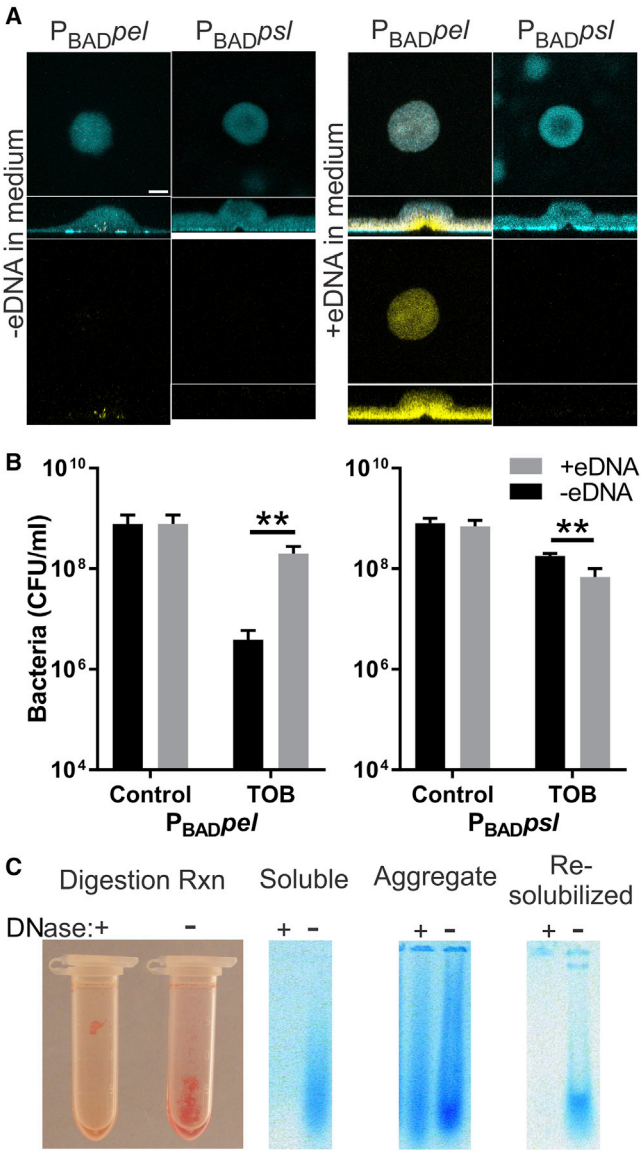


Figure 4. Pel-eDNA interactions enhance bacterial tolerance to aminoglycoside antibiotics and resist nuclease digestion

(A) Pel-dependent biofilms retain more eDNA than Psl-dependent biofilms. Representative confocal microscopy images of extracellular DNA stained with propidium iodide (yellow) and biomass stained with SYTO62 (cyan). Scale bar, 30 μm.

(B) eDNA enhances tolerance to tobramycin (TOB) in a Pel-dependent manner. Plots show viable bacterial counts from static biofilms treated with TOB compared with no antibiotic controls. Results are the mean ± SD (n = 3), p value = 0.0048 and 0.0049 for Pel and Psl, respectively.

(C) Pel protects DNA from nuclease digestion. Image shows Pel-DNA aggregates after 48-h DNase digestion. Ethidium-bromide-stained agarose gel shows DNA (blue) from sonicated Pel-DNA aggregate and soluble portion. Re-solubilizing the aggregates by increasing the pH to disrupt ionic interactions enables digestion with DNase. Representative images shown for clarity. Biological replicate behaved similarly.

Pel interactions with host-airway components reduce *P. aeruginosa*'s susceptibility to antibiotic and mucolytic treatments

CF airways are rich in eDNA, which can be incorporated into the *P. aeruginosa* biofilm matrix (Moreau-Marquis et al., 2008; Walker et al., 2005). To determine whether the biofilm matrix composition impacts the ability of aggregates to incorporate eDNA, we tested *in-vitro*-grown biofilms using either Pel- or Psl-rich matrices in growth medium supplemented with salmon sperm DNA. Propidium iodide (PI) staining of eDNA showed that biofilms overexpressing Pel incorporated large amounts of DNA throughout the biofilm matrix, while DNA observed in Psl overexpression biofilms was near background levels (Figure 4A).

We then assessed whether Pel-bound eDNA might influence antibiotic susceptibility. Colvin et al. (2011) demonstrated that Pel enhances tolerance to the aminoglycoside antibiotic tobramycin, while Psl did not affect susceptibility. Protection only occurred with the charged antibiotic tobramycin and not the neutral antibiotic ciprofloxacin. We cultivated static Pel- or Psl-rich biofilms in medium supplemented with or without eDNA (Figure 4B). We found that Pel-rich biofilms supplemented with eDNA showed decreased susceptibility to tobramycin. This is consistent with the observation that eDNA increases tolerance to aminoglycosides (Chiang et al., 2013).

A feature of EPS interactions is that they protect polymers from enzymatic degradation (Reichhardt et al., 2018). One common treatment for CF patients is the application of aerosolized recombinant human deoxyribonuclease I (rhDNase I) to digest eDNA that, in turn, reduces sputum viscosity and improves airway clearance and lung function (Frederiksen et al., 2006; Shak et al., 1990). Thus, we explored whether Pel-eDNA interactions might protect the DNA from nuclease digestion. To test this, Pel-eDNA aggregates were formed by mixing supernatant from a Pel-overproducing culture with salmon sperm DNA and adjusting the pH to 6.3 to induce aggregation. We found that Pel-DNA aggregates resisted digestion with DNase I even after extended digestion (Figure 4C). Re-solubilizing the aggregates by sonication or increasing the pH to disrupt ionic interactions between Pel and eDNA rendered the eDNA DNase sensitive. Taken together, the data suggest that Pel-eDNA interactions will not only promote tobramycin tolerance but also shield aggregates from disruption by nucleases.

DISCUSSION

A key unanswered question in the field of CF microbiology relates to why aggressive antibiotic treatments are ineffective at eradicating established *P. aeruginosa* infections. These chronic infections persist even after initiation of highly effective CFTR modulator therapy (Hisert et al., 2017); thus, a better understanding of how *P. aeruginosa* eludes killing by both host immune factors and antibiotics remains a critical area of research. Physical disruption of *P. aeruginosa* aggregates in laboratory experiments can restore susceptibility to killing with antibiotics (Alhede et al., 2011) and cells of the immune system (Jensen et al., 1992; Kharazmi, 1991). Thus, understanding mechanisms that promote cellular aggregation is an important focus of research efforts.

To investigate whether aggregates observed in CF have features of a matrix-dependent mechanism of formation, we developed a method to directly visualize the biofilm matrix in CF sputum using IHC with antibodies targeting Pel and Psl polysaccharides. Our results illustrate that *in vivo* aggregates found in CF appear to share some of the properties of commonly studied *in vitro* biofilms. We found evidence that both Psl and Pel are produced and can be found associated with these aggregates. The directional orientation and packing of *P. aeruginosa* cells within aggregates is consistent with aggregation by the bridging of matrix polysaccharides. Additional findings indicate that aggregate matrix composition can vary from patient to patient with some containing Pel and others containing both Pel and Psl. Our work is consistent with aggregation in the CF airways being mediated by a bacterially produced matrix of Pel and/or Psl.

There are several limitations of this study. First, IHC was the primary line of evidence used for the detection of Pel and Psl. We undertook significant efforts to ensure that the antibodies were specific to their target antigens by applying appropriate controls and showing that the presence/absence of IHC targets was consistent with DNA evidence from PCR. In addition to detection of Pel and Psl by IHC, the presence of matrix polysaccharides was also supported by the observation of cells aggregating by a bridging mechanism of matrix polysaccharides as opposed to a matrix-independent mechanism. Second, sputum sample sizes were small and limit the extension of our results. The vast majority of *P. aeruginosa* aggregates found in sputum appear to produce Pel or Psl. It is possible that some *in vivo* aggregates do not contain Pel or Psl, but they were not detected in our small patient cohort. Finally, there is evidence that mucoid strains can also produce Pel and Psl. Whether alginate produced by aggregates from patients harboring mucoid strains influenced Pel and Psl staining and localization is unclear.

Evidence that *P. aeruginosa* produces Pel during infection is potentially significant. At a CF-airway-relevant pH, Pel retains a positive charge and can interact with many of the abundant, negatively charged, host-derived compounds found in the airways, such as eDNA. We show two mechanisms by which Pel-eDNA complexes could impact disease. First, Pel-dependent biofilms sequester eDNA in the matrix, which increases tolerance to the aminoglycoside antibiotic tobramycin. This is consistent with a study that showed eDNA could mediate antibiotic tolerance to biofilm aggregates (Wilton et al., 2015). Second, Pel binding to eDNA protects it from DNase digestion. Currently, a major therapeutic used to treat CF is called Pulmozyme, which consists primarily of aerosolized, inhaled DNase and is meant to reduce airway secretion viscosity by degrading the eDNA-rich airway secretions.

This study sheds light on the nature of aggregation *in vivo*. Our findings are supportive of a role for Pel and/or Psl in aggregation of *P. aeruginosa* in disease. *In vitro*, Pel is only expressed when *P. aeruginosa* is grown as a biofilm, where it promotes cellular aggregation (Colvin et al., 2011). However, our results do not rule out the possibility that multiple mechanisms might contribute to the aggregation of *P. aeruginosa* in different areas/environments within the CF airways. In addition to bacterial cells, Pel is also capable of aggregating mucin, eDNA, and CF sputum. We also show that eDNA-Pel interactions have the potential to reduce the efficacy of two therapeutics commonly used in clinic: Pulmozyme (DNase) and tobramycin. Collectively, our work supports the matrix-driven aggregation hypothesis and suggests that targeting matrix-host compound interactions may be an important step toward improving currently used treatments in the clinic.

STAR★METHODS

Detailed methods are provided in the online version of this paper and include the following:

- KEY RESOURCES TABLE
- RESOURCE AVAILABILITY
  - Lead contact
  - Materials availability
  - Data and code availability
- EXPERIMENTAL MODEL AND SUBJECT DETAILS
  - Bacterial Strains and Growth Conditions
  - Sputum Sample Collection and Processing
- METHOD DETAILS
  - Detection of Pel and Psl Genes in Sputum
  - IHC
  - Polysaccharide Isolation for NMR
  - Solid-state NMR
  - Polymer Binding Assay
  - DNase Digestion of Pel/DNA Aggregates
  - Flow-Cell Biofilm and Confocal Microscopy
  - Antimicrobial Tolerance in Biofilm Assay
- QUANTIFICATION AND STATISTICAL ANALYSIS
  - Antibiotic Susceptibility
  - IHC Image Analysis

SUPPLEMENTAL INFORMATION

Supplemental information can be found online at https://doi.org/10.1016/j.celrep.2021.108782.

ACKNOWLEDGMENTS

This work was supported by NIH grants 5R01AI077628 (M.R.P. and D.J.W.), R01AI143916 (M.R.P. and D.J.W.), R01AI134895 (M.R.P. and D.J.W.), and in part by P20GM103546 and R01AI138981 (P.R.S.), and CFF grant PARSEK17IO (M.R.P.). L.K.J. is the recipient of an AHA fellowship (14POST20130017). C.R. is the recipient of an NIH K99 (5K99GM134121-02) and CFF award (REICHH19F5). We thank Lynette Cegelski for NMR spectrometer access.

AUTHOR CONTRIBUTIONS

L.K.J. and M.R.P. wrote the manuscript. L.K.J., J.E.D., C.R., K.M.S., P.R.S., D.J.W., K.B.H., and M.R.P. designed experiments. L.K.J., J.E.D., C.R., K.M.S., and K.B.H. performed experiments.

DECLARATION OF INTERESTS

The authors declare no conflicts of interests.

Received: September 21, 2020
Revised: January 18, 2021
Accepted: February 2, 2021
Published: February 23, 2021

REFERENCES

Alhede, M., Kragh, K.N., Qvortrup, K., Allesen-Holm, M., van Gennip, M., Christensen, L.D., Jensen, P.Ø., Nielsen, A.K., Parsek, M., Wozniak, D., et al. (2011). Phenotypes of non-attached *Pseudomonas aeruginosa* aggregates resemble surface attached biofilm. PLoS ONE *6*, e27943.

Bjarnsholt, T., Jensen, P.Ø., Fiandaca, M.J., Pedersen, J., Hansen, C.R., Andersen, C.B., Pressler, T., Givskov, M., and Høiby, N. (2009). *Pseudomonas aeruginosa* biofilms in the respiratory tract of cystic fibrosis patients. Pediatr. Pulmonol. *44*, 547–558.

Bjarnsholt, T., Alhede, M., Alhede, M., Eickhardt-Sørensen, S.R., Moser, C., Kühl, M., Jensen, P.Ø., and Høiby, N. (2013). The *in vivo* biofilm. Trends Microbiol. *21*, 466–474.

Borlee, B.R., Goldman, A.D., Murakami, K., Samudrala, R., Wozniak, D.J., and Parsek, M.R. (2010). *Pseudomonas aeruginosa* uses a cyclic-di-GMP-regulated adhesin to reinforce the biofilm extracellular matrix. Mol. Microbiol. *75*, 827–842.

Button, B., Cai, L.-H., Ehre, C., Kesimer, M., Hill, D.B., Sheehan, J.K., Boucher, R.C., and Rubinstein, M. (2012). A periciliary brush promotes the lung health by separating the mucus layer from airway epithelia. Science *337*, 937–941.

Byrd, M.S., Pang, B., Mishra, M., Swords, W.E., and Wozniak, D.J. (2010). The *Pseudomonas aeruginosa* exopolysaccharide Psl facilitates surface adherence and NF-kappaB activation in A549 cells. MBio *1*, e00140–10.

Byrd, M.S., Sadovskaya, I., Vinogradov, E., Lu, H., Sprinkle, A.B., Richardson, S.H., Ma, L., Ralston, B., Parsek, M.R., Anderson, E.M., et al. (2009). Genetic and biochemical analyses of the *Pseudomonas aeruginosa* Psl exopolysaccharide reveal overlapping roles for polysaccharide synthesis enzymes in Psl and LPS production. Mol. Microbiol. *73*, 622–638.

Cantin, A.M., Hartl, D., Konstan, M.W., and Chmiel, J.F. (2015). Inflammation in cystic fibrosis lung disease: Pathogenesis and therapy. J. Cyst. Fibros. *14*, 419–430.

Chiang, W.-C., Nilsson, M., Jensen, P.Ø., Høiby, N., Nielsen, T.E., Givskov, M., and Tolker-Nielsen, T. (2013). Extracellular DNA shields against aminoglycosides in *Pseudomonas aeruginosa* biofilms. Antimicrob. Agents Chemother. *57*, 2352–2361.

Coakley, R.D., Grubb, B.R., Paradiso, A.M., Gatzy, J.T., Johnson, L.G., Kreda, S.M., O'Neal, W.K., and Boucher, R.C. (2003). Abnormal surface liquid pH regulation by cultured cystic fibrosis bronchial epithelium. Proc. Natl. Acad. Sci. USA *100*, 16083–16088.

Colvin, K.M., Gordon, V.D., Murakami, K., Borlee, B.R., Wozniak, D.J., Wong, G.C.L., and Parsek, M.R. (2011). The pel polysaccharide can serve a structural and protective role in the biofilm matrix of *Pseudomonas aeruginosa*. PLoS Pathog. *7*, e1001264.

Colvin, K.M., Irie, Y., Tart, C.S., Urbano, R., Whitney, J.C., Ryder, C., Howell, P.L., Wozniak, D.J., and Parsek, M.R. (2012). The Pel and Psl polysaccharides provide *Pseudomonas aeruginosa* structural redundancy within the biofilm matrix. Environ. Microbiol. *14*, 1913–1928.

Colvin, K.M., Alnabelseya, N., Baker, P., Whitney, J.C., Howell, P.L., and Parsek, M.R. (2013). PelA deacetylase activity is required for Pel polysaccharide synthesis in *Pseudomonas aeruginosa*. J. Bacteriol. *195*, 2329–2339.

Costerton, J.W., Lewandowski, Z., Caldwell, D.E., Korber, D.R., and Lappin-Scott, H.M. (1995). Microbial biofilms. Annu. Rev. Microbiol. *49*, 711–745.

Dorken, G., Ferguson, G.P., French, C.E., and Poon, W.C. (2012). Aggregation by depletion attraction in cultures of bacteria producing exopolysaccharide. J. R. Soc. Interface *9*, 3490–3502.

Fischer, H., and Widdicombe, J.H. (2006). Mechanisms of acid and base secretion by the airway epithelium. J. Membr. Biol. *211*, 139–150.

Flemming, H.-C., and Wingender, J. (2010). The biofilm matrix. Nat. Rev. Microbiol. *8*, 623–633.

Franklin, M.J., Nivens, D.E., Weadge, J.T., and Howell, P.L. (2011). Biosynthesis of the *Pseudomonas aeruginosa* extracellular polysaccharides, alginate, Pel, and Psl. Front. Microbiol. *2*, 167.

Frederiksen, B., Pressler, T., Hansen, A., Koch, C., and Høiby, N. (2006). Effect of aerosolized rhDNase (Pulmozyme) on pulmonary colonization in patients with cystic fibrosis. Acta Paediatr. *95*, 1070–1074.

Gibson, R.L., Burns, J.L., and Ramsey, B.W. (2003). Pathophysiology and management of pulmonary infections in cystic fibrosis. Am. J. Respir. Crit. Care Med. *168*, 918–951.

Hisert, K.B., Heltshe, S.L., Pope, C., Jorth, P., Wu, X., Edwards, R.M., Radey, M., Accurso, F.J., Wolter, D.J., Cooke, G., et al. (2017). Restoring cystic fibrosis transmembrane conductance regulator function reduces airway bacteria and inflammation in people with cystic fibrosis and chronic lung infections. Am. J. Respir. Crit. Care Med. *195*, 1617–1628.

Irie, Y., Borlee, B.R., O'Connor, J.R., Hill, P.J., Harwood, C.S., Wozniak, D.J., and Parsek, M.R. (2012). Self-produced exopolysaccharide is a signal that stimulates biofilm formation in *Pseudomonas aeruginosa*. Proc. Natl. Acad. Sci. USA *109*, 20632–20636.

Jennings, L.K., Storek, K.M., Ledvina, H.E., Coulon, C., Marmont, L.S., Sadovskaya, I., Secor, P.R., Tseng, B.S., Scian, M., Filloux, A., et al. (2015). Pel is a cationic exopolysaccharide that cross-links extracellular DNA in the *Pseudomonas aeruginosa* biofilm matrix. Proc. Natl. Acad. Sci. USA *112*, 11353–11358.

Jensen, E.T., Kharazmi, A., Høiby, N., and Costerton, J.W. (1992). Some bacterial parameters influencing the neutrophil oxidative burst response to *Pseudomonas aeruginosa* biofilms. APMIS *100*, 727–733.

Kharazmi, A. (1991). Mechanisms involved in the evasion of the host defence by *Pseudomonas aeruginosa*. Immunol. Lett. *30*, 201–205.

Little, D.J., Li, G., Ing, C., DiFrancesco, B.R., Bamford, N.C., Robinson, H., Nitz, M., Pomès, R., and Howell, P.L. (2014). Modification and periplasmic translocation of the biofilm exopolysaccharide poly-β-1,6-*N*-acetyl-*D*-glucosamine. Proc. Natl. Acad. Sci. USA *111*, 11013–11018.

Lyczak, J.B., Cannon, C.L., and Pier, G.B. (2002). Lung infections associated with cystic fibrosis. Clin. Microbiol. Rev. *15*, 194–222.

Ma, L., Jackson, K.D., Landry, R.M., Parsek, M.R., and Wozniak, D.J. (2006). Analysis of *Pseudomonas aeruginosa* conditional Psl variants reveals roles for the Psl polysaccharide in adhesion and maintaining biofilm structure postattachment. J. Bacteriol. *188*, 8213–8221.

Mishra, M., Byrd, M.S., Sergeant, S., Azad, A.K., Parsek, M.R., McPhail, L., Schlesinger, L.S., and Wozniak, D.J. (2012). *Pseudomonas aeruginosa* Psl polysaccharide reduces neutrophil phagocytosis and the oxidative response by limiting complement-mediated opsonization. Cell. Microbiol. *14*, 95–106.

Moreau-Marquis, S., Stanton, B.A., and O'Toole, G.A. (2008). *Pseudomonas aeruginosa* biofilm formation in the cystic fibrosis airway. Pulm. Pharmacol. Ther. *21*, 595–599.

Mrsny, R.J., Daugherty, A.L., Short, S.M., Widmer, R., Siegel, M.W., and Keller, G.-A. (1996). Distribution of DNA and alginate in purulent cystic fibrosis sputum: implications to pulmonary targeting strategies. J. Drug Target. *4*, 233–243.

Pamp, S.J., Gjermansen, M., and Tolker-Nielsen, T. (2007). The biofilm matrix: a sticky framework. In The biofilm mode of life: mechanisms and adaptations, S. Kjelleberg and M. Givskov, eds. (Horizon Bioscience), pp. 37–69.

Reichhardt, C., Wong, C., Passos da Silva, D., Wozniak, D.J., and Parsek, M.R. (2018). CdrA interactions within the *Pseudomonas aeruginosa* biofilm matrix safeguard it from proteolysis and promote cellular packing. MBio *9*, e01376, e01318.

Schwarz-Linek, J., Dorken, G., Winkler, A., Wilson, L., Pham, N., French, C., Schilling, T., and Poon, W. (2010). Polymer-induced phase separation in suspensions of bacteria. EPL *89*, 68003.

Secor, P.R., Michaels, L.A., Ratjen, A., Jennings, L.K., and Singh, P.K. (2018). Entropically driven aggregation of bacteria by host polymers promotes antibiotic tolerance in *Pseudomonas aeruginosa*. Proc. Natl. Acad. Sci. USA *115*, 10780–10785.

Secor, P.R., Sweere, J.M., Michaels, L.A., Malkovskiy, A.V., Lazzareschi, D., Katznelson, E., Rajadas, J., Birnbaum, M.E., Arrigoni, A., Braun, K.R., et al.

(2015). Filamentous bacteriophage promote biofilm assembly and function. Cell Host Microbe *18*, 549–559.

Shak, S., Capon, D.J., Hellmiss, R., Marsters, S.A., and Baker, C.L. (1990). Recombinant human DNase I reduces the viscosity of cystic fibrosis sputum. Proc. Natl. Acad. Sci. USA *87*, 9188–9192.

Singh, P.K., Schaefer, A.L., Parsek, M.R., Moninger, T.O., Welsh, M.J., and Greenberg, E.P. (2000). Quorum-sensing signals indicate that cystic fibrosis lungs are infected with bacterial biofilms. Nature *407*, 762–764.

Somayaji, R., Parkins, M.D., Shah, A., Martiniano, S.L., Tunney, M.M., Kahle, J.S., Waters, V.J., Elborn, J.S., Bell, S.C., Flume, P.A., and VanDevanter, D.R.; Antimicrobial Resistance in Cystic Fibrosis InternationalWorking Group (2019). Antimicrobial susceptibility testing (AST) and associated clinical outcomes in individuals with cystic fibrosis: A systematic review. J. Cyst. Fibros. *18*, 236–243.

Staudinger, B.J., Muller, J.F., Halldórsson, S., Boles, B., Angermeyer, A., Nguyen, D., Rosen, H., Baldursson, O., Gottfreðsson, M., Guðmundsson, G.H., and Singh, P.K. (2014). Conditions associated with the cystic fibrosis defect promote chronic *Pseudomonas aeruginosa* infection. Am. J. Respir. Crit. Care Med. *189*, 812–824.

Stoltz, D.A., Meyerholz, D.K., and Welsh, M.J. (2015). Origins of cystic fibrosis lung disease. N. Engl. J. Med. *372*, 351–362.

Strand, S.P., Vårum, K.M., and Østgaard, K. (2003). Interactions between chitosans and bacterial suspensions: adsorption and flocculation. Colloids Surf. B Biointerfaces *27*, 71–81.

Sutherland, I. (2001). Biofilm exopolysaccharides: a strong and sticky framework. Microbiology (Reading) *147*, 3–9.

Vårum, K.M., Anthonsen, M.W., Grasdalen, H., and Smidsrød, O. (1991). Determination of the degree of *N*-acetylation and the distribution of *N*-acetyl groups in partially *N*-deacetylated chitins (chitosans) by high-field NMR spectroscopy. Carbohydr. Res. *211*, 17–23.

Walker, T.S., Tomlin, K.L., Worthen, G.S., Poch, K.R., Lieber, J.G., Saavedra, M.T., Fessler, M.B., Malcolm, K.C., Vasil, M.L., and Nick, J.A. (2005). Enhanced *Pseudomonas aeruginosa* biofilm development mediated by human neutrophils. Infect. Immun. *73*, 3693–3701.

Wilton, M., Charron-Mazenod, L., Moore, R., and Lewenza, S. (2015). Extracellular DNA acidifies biofilms and induces aminoglycoside resistance in *Pseudomonas aeruginosa*. Antimicrob. Agents Chemother. *60*, 544–553.

STAR★METHODS

KEY RESOURCES TABLE

REAGENT or RESOURCE	SOURCE	IDENTIFIER
Antibodies		
Pseudomonas aeruginosa antibody, guinea pig polyclonal, isotype IgG	GeneTex	GTX41031; RRID:AB_424383
Bacterial and virus strains		
PAO1 Δ*wspF* Δ*pel* P_{BAD}*psl* - arabinose-inducible *psl* operon	Irie et al., 2012	N/A
PAO1 Δ*wspF* Δ*psl* P_{BAD}*pel* - *wspF*, nonpolar mutation; *pslBCD*, polar mutant of the *psl* operon; arabinose-inducible *pel* operon	Colvin et al., 2013	N/A
PAO1 Δ*wspF* Δ*psl* Δ*pel* - *wspF*, nonpolar mutation; *pelA*, polar mutant of the *pel* operon; *pslBCD*, polar mutant of the *psl* operon	Borlee et al., 2010	N/A
Chemicals, peptides, and recombinant proteins		
Sodium alginate	Sigma-Aldrich	W201502; CAS: 9005-38-3
DNA, salmon sperm	USB	14377
Congo red	Sigma-Aldrich	C6767
SYTO 62 red fluorescent nucleic-acid stain	Thermo Fisher	S11344
Propidium iodide (PI)	Thermo Fisher	BMS500PI
Triton X-100 detergent	Roche	11332481001; CAS: 9002-93-1
Harris hematoxylin	Leica Biosystems	3801562
GoTaq Flexi DNA polymerase	Promega	M8291
DNase I, recombinant RNase-free	Sigma-Aldrich	4716728001
Proteinase K	New England Biolabs	P8107S
Critical commercial assays		
QIAamp DNA Microbiome Kit	QIAGEN	19091
Oligonucleotides		
Pa-rplU-F: CGT CAC GAC AAG GTC CGC	Secor et al., 2015	N/A
Pa-rplU-R: GGC CTG AAT GCC GGT GAT C	Secor et al., 2015	N/A
pelA-F: CCT TCA GCC ATC CGT TCT	Colvin et al., 2011	N/A
pelA-R: TCG CGT ACG AAG TCG ACC TT	Colvin et al., 2011	N/A
pslA-F: CTG CCC TCA CCT TTC GCC	This Study	N/A
pslA-R: GGA AGG ATC AGC TGC G	This Study	N/A
Software and algorithms		
Igor Pro	WaveMetrics	https://www.wavemetrics.com/products/igorpro
Velocity	Quorum Technologies	www.quorumtechnologies.com
Prism	GraphPad	https://www.graphpad.com:443/
VisioPharm Image Analysis Software	VisioPharm	https://www.visiopharm.com/

CellPress
OPEN ACCESS

RESOURCE AVAILABILITY

Lead contact

Further information and requests for reagents may be directed to, and will be fulfilled by, the corresponding author Dr. Matthew Parsek (parsem@u.washington.edu).

Materials availability

This study did not generate unique reagents.

Data and code availability

This study did not generate unique datasets or code.

EXPERIMENTAL MODEL AND SUBJECT DETAILS

Bacterial Strains and Growth Conditions

Bacterial strains and primers used in this study are listed in the Key Resources Table (Borlee et al., 2010; Colvin et al., 2011, 2013; Irie et al., 2012; Secor et al., 2015). Planktonic cultures were routinely cultivated on Jensen's chemically defined medium at 37°C with constant shaking (225 rpm) unless otherwise indicated. Jensen's medium (pH 7.3) contained NaCl (85.6 mM), K_2HPO_4 (14.4 mM), sodium glutamate (92 mM), valine (24 mM), phenylalanine (8 mM), glucose (70 mM), $MgSO_4$ (1.33 mM), $CaCl_2$ (0.14 mM), $FeSO_4$ (0.0039 mM), and $ZnSO_4$ (0.0085 mM). The first five ingredients were mixed, the pH was adjusted to 7.3, and the resulting solution was subsequently autoclaved. Jensen's medium was supplemented with glucose and metals after autoclaving. Biofilms were cultivated on glucose minimal media (pH 7), which was made by modifying the Jensen's glucose recipe as follows: the glucose concentration was reduced to 0.3 mM, ammonium sulfate was added (15.1 mM final concentration), and the amino acids valine, phenylalanine, and glutamic acid were removed. Media for induced strains was supplemented with arabinose at 0.5% (vol/vol).

Sputum Sample Collection and Processing

Spontaneously expectorated sputum specimens were collected at the University of Washington (UW) Adult Cystic Fibrosis Clinic and kept on ice (0.5 - 4 hours) until processing. Informed consent was obtained from all subjects, and the study was approved by the UW Human Subjects Division. Patient identification number, age, forced expiratory volume (FEV1), clinical lab microbiology, and cystic fibrosis transmembrane conductance regulator (CFTR) genotype are indicated in Table S1. Sex and gender identity for patients is not known. For each sputum sample, part was fixed in formalin for IHC analysis, part was used to extract bacterial DNA, and the remaining sample was frozen at −20°C.

METHOD DETAILS

Detection of Pel and Psl Genes in Sputum

Bacterial DNA was extracted directly from fresh expectorated sputum using a QIAamp DNA Microbiome Kit (QIAGEN) to reduce contamination with human DNA. Endpoint PCR was used to confirm clinical findings that sputum samples were *P. aeruginosa* positive or negative and to determine if *pel* or *psl* genes were present. PCR was performed using GoTaq® Flexi DNA polymerase (Promega) according to the manufacturer's instructions with primers specific for Pel (*pelA*-F, *pelA*-R), Psl (*pslA*-F, *pslA*-R), and *P. aeruginosa* (PA-*rplU*-F, PA-*rplU*-R) (see Key resources table). An annealing temperature of 61°C was used for each of the PCR reactions.

IHC

IHC targeting Pel, Psl, and *P. aeruginosa* was performed by the Histology and Imaging Core Facility at UW. Following expectoration, sputum samples were placed in 50 mL conical vials containing 10% formalin. Fixed specimens were embedded in paraffin and sectioned. 5 μm sections were collected and placed onto charged slides, deparaffinized and rehydrated through graded ethanol. The signal-to-noise ratio for each antibody was optimized by varying the antigen retrieval and primary antibody concentration. Antigen retrieval was performed with citrate buffer at pH 6 for 10 minutes followed by blocking with endogenous peroxidase activity with 3.0% hydrogen peroxide for 5 minutes. The sections were incubated with rabbit anti-Pel antisera, rabbit anti-Psl antisera, guinea pig anti-*Pseudomonas aeruginosa* antisera (GeneTex) or rabbit non-specific control IgGs. Antisera for *P. aeruginosa*, Pel, and Psl was applied at 1:5000, 1:60, and 1:2000 dilutions, respectively. Sections were washed, incubated with secondary antibodies conjugated to horseradish peroxidase. Counter-staining was performed using Harris hematoxylin (Leica Biosystems).

Antibodies for IHC were validated using positive and negative controls. Negative controls consisted of sputum without *P. aeruginosa*. PCR confirmed that negative controls did not contain *P. aeruginosa*, *pel* or *psl* genes. To create positive controls, 100 ul of a 16-hour culture of a Pel or Psl overproducing strain cultivated in Jensen's minimal media was spiked into sputum without *P. aeruginosa* (Figures S2A and S2B). The sputum with culture was allowed to stand for an hour at room temperature prior to fixing in formalin for IHC analysis. Sputum without *P. aeruginosa* did not demonstrate robust staining with Pel or Psl antibodies. Some

non-specific binding to abiotic material and host cells was observed in controls and could be distinguished from matrix staining which co-localized with anti-*P. aeruginosa* staining of cell aggregates. Sputum exogenously spiked with cultures that overproduce Pel or Psl showed the presence of rod-shaped bacteria associated with Pel and Psl staining. Variability was noted between sputum samples both in composition and staining. Some samples contained large amounts of saliva, while others relatively little. The *P. aeruginosa* antibody (GeneTex) targeted *P. aeruginosa* outer membrane protein fraction and could not be applied to some *P. aeruginosa*-containing samples due to high background staining.

Polysaccharide Isolation for NMR

Crude preparations of Pel and Psl polysaccharides were prepared by harvesting the supernatant from strains engineered to overproduce Pel or Psl in the presence of arabinose. Jensen's medium was inoculated with 1 mL of overnight culture of the Pel overexpression strain PAO1 Δ*wspF* Δ*psl* P_{BAD} *pel* or Psl overexpression strain PAO1 Δ*wspF* Δ*pel* P_{BAD} *psl* (Jennings et al., 2015). Cultures were grown for 20 h at 37°C with constant shaking. To obtain secreted Pel or Psl, the supernatant was harvested by centrifugation (8,300 x g for 15 min at 20°C).

Secreted Pel polysaccharides from culture supernatant were precipitated for 1 h at 4°C with ethanol (final concentration 75% v/v). The precipitate was washed three times with 95%–100% (v/v) ethanol, resuspended in 20 mL of buffer (1 mM $CaCl_2$ and 2 mM $MgCl_2$ in 50 mM Tris, pH 7.5), and treated with 100 mg DNase I (Sigma Aldrich) overnight at 37°C, followed by 100 mg of proteinase K (NEB) overnight at 37°C. Sodium dodecyl sulfate (SDS) was added to the enzyme-treated samples at a final concentration of 4% (w/v) and heated to 95°C for 10 min. The polysaccharide sample was centrifuged at 8,300 x g for 15 min at 20°C, and the resulting pellet was resuspended in water. The water washing step was repeated until the SDS was removed. The polysaccharides were precipitated again for 1 h at 4°C with ethanol (final concentration 75% v/v). The samples were extensively dialyzed against water (100 kDa molecular-weight cut off), and then flash-frozen and lyophilized for NMR analysis.

Solid-state NMR

All solid-state NMR experiments were performed using an 89-mm wide-bore Varian magnet at 11.7 T (499.12 MHz for ^{1}H, 125.52 MHz for ^{13}C, and 50.58 MHz for ^{15}N) and an 89-mm wide-bore Agilent magnet at 11.7 T (500.92 MHz for ^{1}H, 125.97 MHz for ^{13}C, and 50.76 MHz for ^{15}N), Varian/Agilent consoles, and home-built four-frequency transmission-line probes with a 13.66 mm long, 6-mm-inner-diameter sample coil and a Revolution NMR MAS Vespel stator. Samples were spun in thin-wall 5-mm-outer-diameter zirconia rotors (Revolution NMR, LLC) at 7,143 ± 2 Hz, using a Varian MAS control unit. The temperature was maintained at −10°C. For all NMR experiments, π-pulse lengths were 7 μs for ^{1}H and 10 μs for ^{13}C. Proton-carbon cross-polarization occurred at 50 kHz for 1.5 ms unless otherwise noted. Proton dipolar coupling was performed at 90 kHz with TPPM modulation. The chemical shift of ^{13}C spectra was referenced to external adamantane. Multi-peak fitting and integration was performed in software written for Igor Pro (WaveMetrics, Lake Oswego, OR, USA).

To confirm the polysaccharide composition and to assess the degree of deacetylation, we applied solid-state NMR to Pel from an overproducing strain P_{BAD}*pel* (Jennings et al., 2015). The ^{13}C cross-polarization magic-angle spinning (^{13}C-CPMAS) NMR spectrum of secreted Pel was acquired. To determine the extent of Pel deacetylation, the cross-polarization (CP) contact time was arrayed, which permitted quantitative peak integration.

Polymer Binding Assay

To determine if *P. aeruginosa* EPS other than Pel could ionically bind exogenous DNA, a method was used similar to that outlined in Jennings et al. (2015). Sodium alginate (5 mg/ml, Sigma W201502) and culture supernatant (1.5 ml) from Pel or Psl overproducing strains and a Δ*pel* Δ*psl* deletion mutant were combined with salmon sperm DNA (5 mg/ml, USB 14377). Samples were vortexed, placed on a rotator for at least 20 minutes and drawn through a 22-gauge needle to ensure that polymers were fully in solution. To induce aggregation, the pH of the EPS/DNA solution was adjusted to 6.3 or 7.3 by the addition of 1 N HCl. Congo Red (Sigma-Aldrich, C6767, 40 μg/ml final concentration) was added to enhance visualization of aggregates, although unstained samples behaved similarly.

To test for interactions between Pel and sputum, supernatant from Pel and Psl overexpression strains and a Δ*pel* Δ*psl* deletion mutant (1.4 ml) was mixed with homogenized sputum (0.1 ml). The pH of the corresponding solutions was adjusted to 6.3 and 7.3.

DNase Digestion of Pel/DNA Aggregates

To determine if Pel/DNA aggregates resisted nuclease digestion, Pel/DNA aggregates were formed by mixing supernatant from a Pel overexpression culture with 5 mg/ml DNA and lowering the pH to 6.3. Aggregates were physically removed and placed in a buffer (1 mM $CaCl_2$ and 2 mM $MgCl_2$ in 50 mM Tris, pH 7.5) with or without DNase I (Sigma-Aldrich, 20 μg/ml). Digestion was carried out at 37°C for 1 hour or up to 48 h. Congo Red was added prior to imaging. Half of the aggregates were broken-up by sonication in 50 μl of water. The sonicated aggregate and the soluble portion of the enzyme digest reaction was run on a 1% agarose gel to detect DNA in the samples.

Flow-Cell Biofilm and Confocal Microscopy

Biofilms were cultivated in flow cell chambers essentially as described by Jennings et al. (2015). Flow cells were inoculated from a mid-log LB culture that was diluted with glucose minimal media to an optical density at 600 nm of 0.01. Strains that aggregated in mid-log phase were homogenized before dilution for inoculation. Cells were allowed to attach under static conditions to an inverted flow cell for 1 h before induction of flow. Biofilms were grown on glucose minimal media supplemented with or without exogenous salmon sperm DNA (USB) at 40 μg/ml for 2 d at room temperature under a constant flow rate (10 mL/h). Biofilms were stained for 15 min with Syto62 red fluorescent nucleic-acid stain (5 μM; ThermoFisher) for biomass and PI (30 μM; ThermoFisher) for eDNA. After staining, flow cells were washed with media at 10 mL/h for 5 min and then visualized on a Zeiss LSM 510 scanning confocal laser microscope. Image analysis was conducted using Velocity software (Quorum Technologies). Microscopy images were artificially colored as follows: Syto62 biomass, cyan; and PI eDNA, yellow.

Antimicrobial Tolerance in Biofilm Assay

Static biofilms were used to measure the effect of eDNA on the sensitivity of P_{BAD} *pel* and P_{BAD} *psl* to tobramycin (Sigma). 48-well plates containing LB with and without exogenous DNA at 100 μg/ml were inoculated with exponentially growing P_{BAD} *pel* and P_{BAD} *psl* cells. Biofilms were cultivated statically for 8 hours at 37°C. At which point, the spent medium was decanted, and biofilms were washed once with phosphate buffered saline solution (PBS) followed by replacement with medium supplemented with or without tobramycin (50 μg/ml). Biofilms were incubated with antibiotic for 30 min at 37°C followed by removal of medium and washing of cells with PBS. After the second washing, biofilms were treated with 0.5% Triton X-100 detergent (Roche) and shaken at room temperature for 30 minutes to dislodge cells from the plate surface. Viable bacterial counts were determined by making serial dilutions into PBS and dropping 10 μl dilutions onto LB agar plates. Colony forming units were counted after overnight incubation at 37°C.

QUANTIFICATION AND STATISTICAL ANALYSIS

Antibiotic Susceptibility

The statistical significance of the effect of DNA on antibiotic susceptibility was determined in Prism (GraphPad) using an unpaired, nonparametric Mann-Whitney test to calculate approximate *p-value*s comparing conditions with and without exogenous DNA. The mean ± SD of three experiments (n = 3 for each experiment) were calculated. A *p-value* less than or equal to 0.05 was considered significant.

IHC Image Analysis

IHC slides were scanned and visualized on a Hamamatsu NanoZoomer Digital Pathology (NDP) System. Images of IHC slides were captured by microscopy. Biofilm aggregate size was estimated in sputum samples containing *P. aeruginosa* by measuring the longest diameter or length directly on scanned IHC slides on aggregates greater than 4 μm. The presence of Pel and Psl in sputum was determined by visual inspection and quantification of antibody signal using VisioPharm image analysis software. A global quantification of antibody signal across the entire slide was normalized to total specimen area.